

Engineering of Unspecific Peroxygenases Using a Superfolder-Green-Fluorescent-Protein-Mediated Secretion System in *Escherichia coli*

Published as part of JACS Au virtual special issue "Biocatalysis in Asia and Pacific".

Xingyu Yan,[†] Xiaodong Zhang,[†] Haoran Li,[†] Di Deng, Zhiyong Guo, Lixin Kang,* and Aitao Li*



Cite This: *JACS Au* 2024, 4, 1654–1663



Read Online

ACCESS |

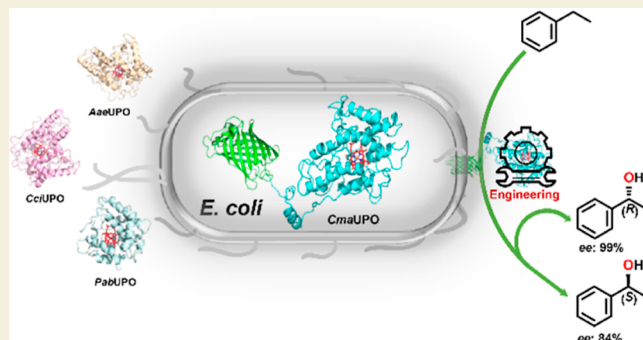
Metrics & More

Article Recommendations

Supporting Information

ABSTRACT: Unspecific peroxygenases (UPOs), secreted by fungi, demonstrate versatility in catalyzing challenging selective oxyfunctionalizations. However, the number of peroxygenases and corresponding variants with tailored selectivity for a broader substrate scope is still limited due to the lack of efficient engineering strategies. In this study, a new unspecific peroxygenase from *Coprinopsis marcescibilis* (*Cma*UPO) is identified and characterized. To enhance or reverse the enantioselectivity of wildtype (WT) *Cma*UPO catalyzed asymmetric hydroxylation of ethylbenzene, *Cma*UPO was engineered using an efficient superfolder-green-fluorescent-protein (*sf*GFP)-mediated secretion system in *Escherichia coli*. Iterative saturation mutagenesis (ISM) was used to target the residual sites lining the substrate tunnel, resulting in two variants: T125A/A129G and T125A/A129V/A247H/T244A/F243G. The two variants greatly improved the enantioselectivities [21% ee (*R*) for WT], generating the (*R*)-1-phenylethanol or (*S*)-1-phenylethanol as the main product with 99% ee (*R*) and 84% ee (*S*), respectively. The *sf*GFP-mediated secretion system in *E. coli* demonstrates applicability for different UPOs (*Aae*UPO, *Cci*UPO, and *Pab*UPO-I). Therefore, this developed system provides a robust platform for heterologous expression and enzyme engineering of UPOs, indicating great potential for their sustainable and efficient applications in various chemical transformations.

KEYWORDS: unspecific peroxygenases, *Cma*UPO, heterologous expression, directed evolution, *sf*GFP, tunnel engineering, generality, application



INTRODUCTION

Unspecific peroxygenases (UPOs, EC 1.11.2.1) are fungal heme-thiolate enzymes that can hydroxylate inactive C–H bonds, epoxidize C=C bonds, and sulfonate thioethers.^{1,2} UPOs only use H₂O₂ as an oxygen and electron donor, without relying on expensive nicotinamide cofactors or electron transport chains,^{3,4} making them superior to P450s.

Since the discovery of the first UPO, *Agrocybe aegerita* (*Aae*UPO) in 2004,⁵ more than 4000 sequences have been annotated as UPOs in BLAST searches of NCBI GenBank and other public sequence databases.⁶ Although a vast diversity of UPO genes are available, only a limited number of UPOs have been purified and experimentally characterized to date, including *Aae*UPO,⁷ *Coprinopsis cinerea* UPO (*Cci*UPO),⁸ *Marasmius rotula* UPO (*Mro*UPO),⁹ *Chaetomium globosum* UPO (*Cgl*UPO),¹⁰ *Collariella virescens* UPO (*Cvi*UPO),¹¹ *Daldinia caldariorum* UPO (*Dca*UPO),¹¹ *Psathyrella aberdarensis* UPO (*Pab*UPO),¹² *Hypoxyylon* sp. EC38 UPO (*Hsp*UPO),¹³ *Galerina marginata* UPO (*Gma*UPO),¹⁴ and *Aspergillus brasiliensis* UPO (*Abr*UPO).¹⁵ In addition, the number of peroxygenase variants with tailored selectivity for a broader range of starting materials is also limited due to the lack of an efficient engineering strategy. The development of a fast and efficient engineering approach for UPOs is highly desired.¹⁶

Currently, several UPOs have undergone directed evolution with *Saccharomyces cerevisiae* (*S. cerevisiae*) as a host to enhance functional expression, catalytic activity, and regioselectivity.^{7,17–19} However, the engineering of UPOs using *S. cerevisiae* is hindered by prolonged heterologous production and the complexity of mutation operations, severely limiting their

Received: February 12, 2024

Revised: March 29, 2024

Accepted: April 1, 2024

Published: April 10, 2024



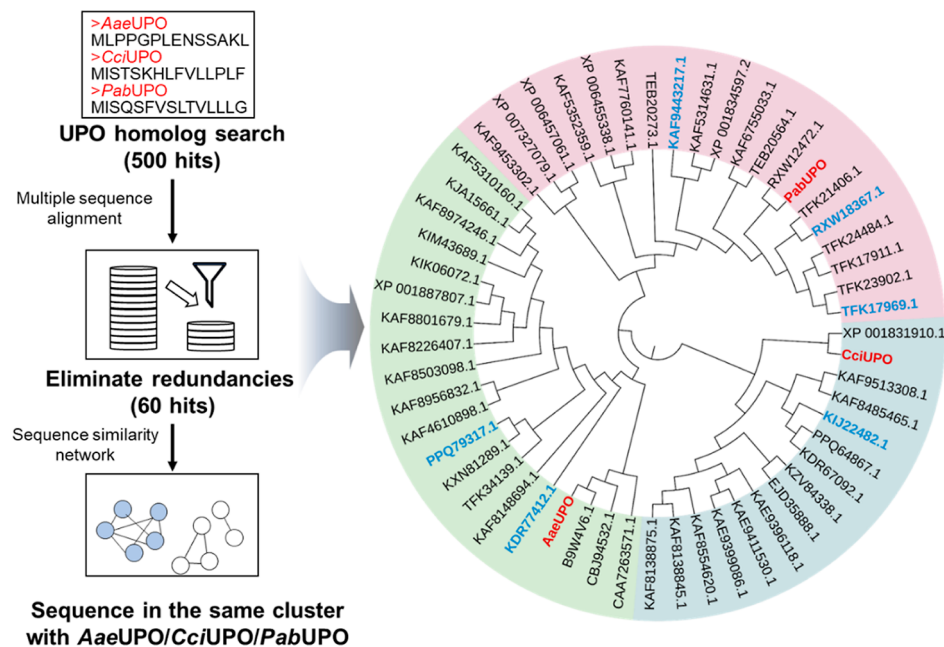


Figure 1. Bioinformatic workflow for the discovery of putative UPOs. Candidate sequences were mined using probes *AaeUPO*, *CciUPO*, and *PabUPO*. A maximum likelihood phylogenetic tree of the UPO candidate referenced the confirmed UPOs, bootstrap values at each node, were from 100 replicates. The probes are highlighted in red, and the UPO candidates selected are marked in blue.

potential for further directed evolution to achieve superior variants. In contrast, *Escherichia coli* (*E. coli*), as one of the most efficient expression hosts, has several advantages such as inexpensive culturing, easy scale-up and short turnaround time, and easy genetic manipulation. However, the heterologous expression of UPOs (originating from fungi) in prokaryotic *E. coli* is challenging. Up to now, only *MroUPO*, *CviUPO*, *DcaUPO*, and *artUPO* (artificial peroxygenase, shares 73% sequence identity with *MroUPO*) have been expressed in soluble and active forms,^{11,20,21} but with very low efficiency. Even worse, complex procedures like codon optimization, autoinduction medium, low incubation temperature, and prolonged induction time (4–5 days) are essential for facilitating the corrected folding of UPOs in *E. coli*.^{11,20} All of these indicated that the current expression system is unsatisfied for engineering of UPOs.

To address the issues, in this study, a novel UPO from *Coprinopsis marcescibilis* (*Cma*UPO) was mined and characterized for diversifying the UPO enzyme toolbox. Then, an efficient superfold green fluorescent protein (*sf*GFP) secretion system in *E. coli* was established for *Cma*UPO expression, which was followed by enzyme engineering to tailor the enantioselectivity of *Cma*UPO catalyzed asymmetric hydroxylation of ethylbenzene. Finally, different types of UPOs were tested with the developed *E. coli* *sf*GFP secretion system to demonstrate its generality, thus laying the foundation for the efficient directed evolution of UPOs for practical applications.

RESULTS AND DISCUSSION

Identification and Characterization of New UPO

To date, only a few UPOs have been identified and characterized, largely due to their poor expression in heterologous hosts.^{22,23} To overcome this limitation, we searched for protein homologues using the amino acid sequences of *AaeUPO* (*A. aegerita*), *CciUPO* (*C. cinerea*), and *PabUPO* (*P. aberdarensis*) as queries against a protein

database. Under limited conditions, we retrieved a total of 500 amino acid sequences and eliminated redundancies to obtain 60 unique sequences. Then, we utilized the Enzyme Similarity Tool (EFI-EST) to generate a sequence similarity network based on the collected candidate sequences. Our focus within this cluster was on identifying UPO candidates that were closely related to *AaeUPO*, *CciUPO*, or *PabUPO*. Based on the information from the phylogenetic tree (Figure 1), we selected six potential UPOs for further characterization. These included *GmaUPO* (*G. marginata* UPO, KDR77412.1) and *PcyUPO* (*Psilocybe cyanescens* UPO, PPQ79317.1), which were clustered in the *AaeUPO* genus. Additionally, *CabUPO* (*Candolleomyces aberdarensis* UPO, RXW18367.1), *CmaUPO* (*C. marcescibilis* UPO, TFK17969.1), and *MfuUPO* (*Macrolepiota fuliginosa* UPO, KAF9443217.1), which were grouped in *PabUPO* clusters, while *SstUPO* (*Sphaerobolus stellatus* UPO, KIJ22482.1) belonged to *CciUPO* clusters.

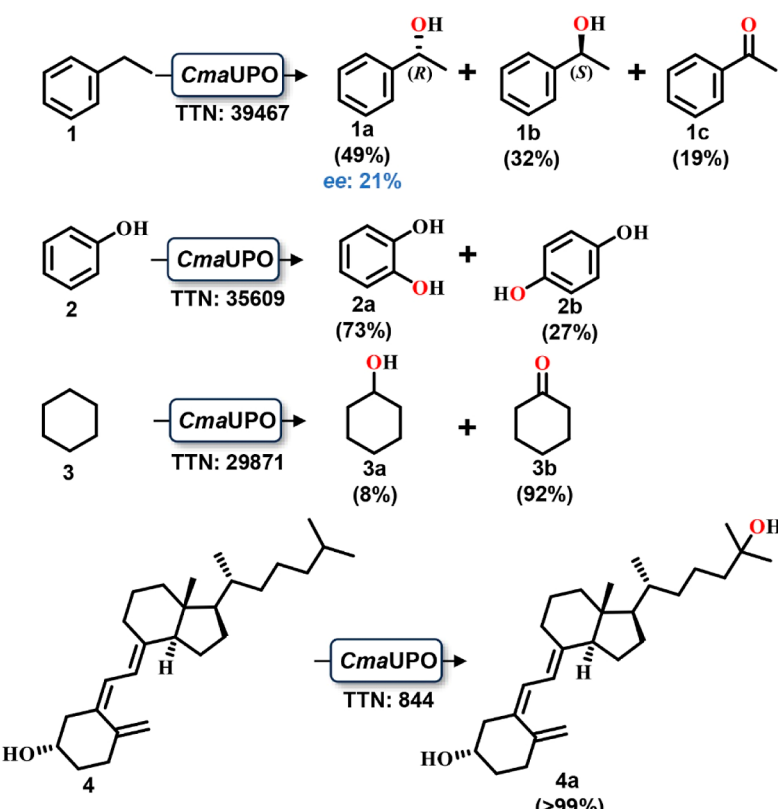
In an initial screening, we synthesized and cloned sequence-optimized genes containing native signal peptides into the pPICZ- α plasmid. Subsequently, we linearized the recombinant plasmids and introduced them into *Pichia pastoris* X33 for expression. Then, we evaluated the peroxidase and peroxygenase activities of the six selected enzymes using two model substrates: ABTS and NBD. Notably, only the enzyme from *C. marcescens* (*CmaUPO*) exhibited obvious activity (394 and 348 U L⁻¹ for ABTS and NBD, respectively) when expressed on a 0.5 L scale (Table S1). Consequently, *CmaUPO* emerged as a primary candidate for further characterization. The molecular weight of *CmaUPO* secreted by recombinant *P. pastoris* was about 50 kDa with a low N-glycosylation degree (Figure S1). In order to assess the impact of reaction conditions on enzyme performance, several experiments were conducted to evaluate the assay pH, temperature, and organic reagent tolerance. It was found that *CmaUPO* displayed optimal activity at pH 7.5 on substrates NBD and veratryl alcohol (VA), and demonstrated good thermal stability at a

Table 1. Steady-State Kinetic Parameter of *CmaUPO* and Other UPOs^a

UPO	substrate	<i>k</i> _{cat} (S ⁻¹)	<i>K</i> _m (μM)	<i>k</i> _{cat} / <i>K</i> _m (S ⁻¹ μM ⁻¹)	reference
<i>CmaUPO</i>	ABTS ^a	76 ± 3	16 ± 3	4.72	this study
	NBD ^b	146 ± 1	241 ± 6	0.61	
	VA ^c	378 ± 5	12,630 ± 609	0.03	
wild-type <i>AaeUPO</i>	ABTS	221 ± 6	25 ± 2	8.8	7
	NBD	219 ± 25	684 ± 207	0.32	
PaDa-I	ABTS	395 ± 13	48 ± 4	8.2	
	NBD	388 ± 22	483 ± 95	0.7	
wild-type <i>PabUPO</i> -I	ABTS	20	105	0.19	12
wild-type <i>PabUPO</i> -II	ABTS	85	128	0.66	
<i>PabUPO</i> -I variant	ABTS	117 ± 2	210 ± 10	0.58	
	NBD	29 ± 1	434 ± 53	0.07	
<i>PabUPO</i> -II variant	ABTS	97 ± 1	243 ± 5	0.68	
	NBD	22 ± 1	354 ± 48	0.06	

^aReaction conditions: 2 mM H₂O₂, 100 mM citric acid/dibasic sodium phosphate pH 4.5 or potassium phosphate pH 7.5, *V*_{final} = 1 mL. All experiments were performed in triplicates. (a) 0–0.2 mM ABTS, 15 nM *CmaUPO*; (b) 0–1.2 mM NBD, 30 nM *CmaUPO*; and (c) 0–100 mM VA, 75 nM *CmaUPO*.

a) Hydroxylation (Alcohol oxidation)



b) Epoxidation

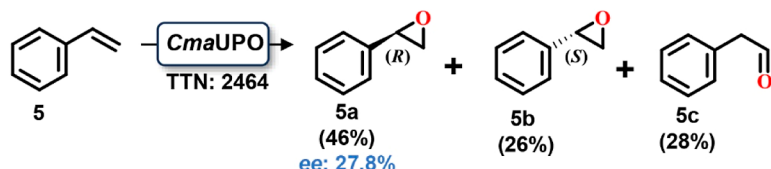


Figure 2. *CmaUPO* substrate panel, with the oxidation sites highlighted. Reaction conditions: substrate (20 mM 1, 50 mM 2, 100 mM 3, 2.5 mM 4, and 10 mM 5), *CmaUPO* (0.15 μM for 1 and 2, 0.3 μM for 3, 1 μM for 4, and 1.5 μM for 5), 25 mM glucose, 100 U mL⁻¹ glucose oxidase, *V*_{final} = 1 mL, 30 °C, 220 rpm, 4 h. Additionally, 5 mM sodium ascorbate was added to substrate 2 to avoid phenoxy radical formation. All experiments were performed in triplicates. Product ratio was determined by the peak area or calibration with the commercial product standards on GC or HPLC.

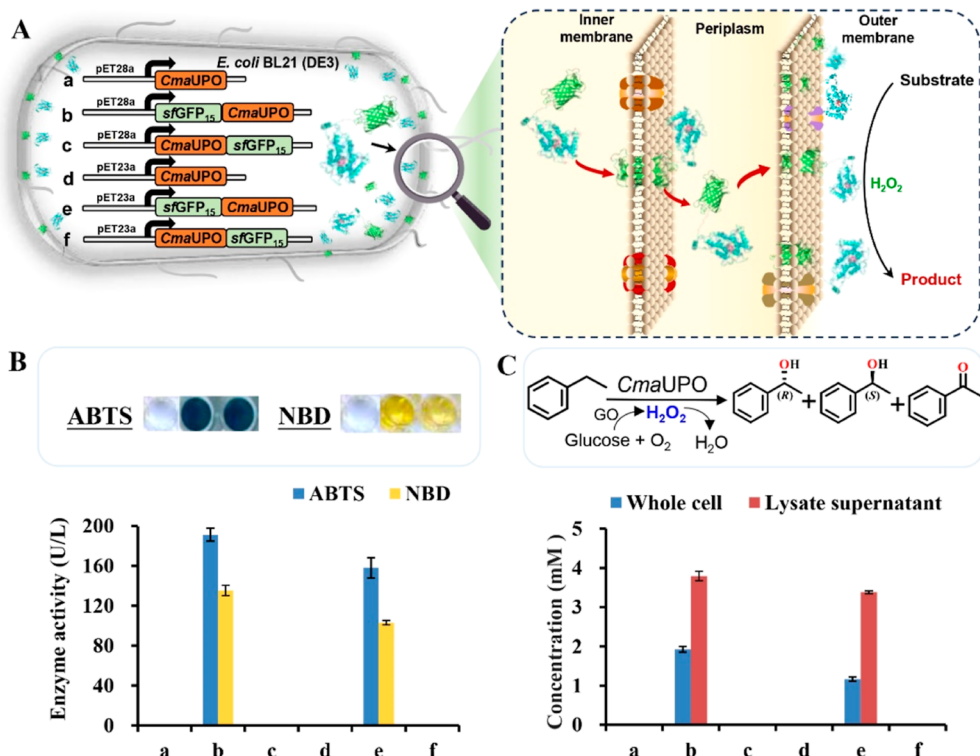


Figure 3. Heterologous expression strategy of *CmaUPO* in *E. coli*. (A) Fusion-expression platform for *CmaUPO* production. *CmaUPO* was fused with sfGFP₁₅ in different plasmid configurations for heterologous expression in *E. coli* BL21 (DE3). Recombinant plasmids: (a) pET28a-*CmaUPO*; (b) pET28a-sfGFP₁₅-*CmaUPO*; (c) pET28a-*CmaUPO*-sfGFP₁₅; (d) pET23a-*CmaUPO*; (e) pET23a-sfGFP₁₅-*CmaUPO*; and (f) pET23a-*CmaUPO*-sfGFP₁₅. (B) Activity test of cell lysates of different recombinant *E. coli* cells expressing *CmaUPO* with ABTS and NBD. (C) Biotransformation catalyzed by the whole cells or lysate of different recombinant *E. coli* cells expressing *CmaUPO* with ethylbenzene as a substrate. Reaction conditions: ethylbenzene 10 mM, *CmaUPO* whole cell ($OD_{600} = 20$, cell dry weight 8 g L⁻¹) or corresponding cell lysate, glucose 25 mM, glucose oxidase 100 U mL⁻¹, 100 mM potassium phosphate pH 7.5, $V_{final} = 1$ mL, 30 °C, 220 rpm, 4 h.

temperature of 30 °C. Furthermore, most solvents showed negative effects on *CmaUPO* activity; however, the NBD activity was boosted to 120% when acetone concentration was 2% (v/v) and residual activity retained about 100% when up to 6.8% (v/v). The optimal concentrations of H₂O₂ for *CmaUPO* activities toward ABTS, NBD, and VA were determined to be 0.5, 3.0, and 0.7 mM, respectively (Figures S2–S7). Furthermore, the kinetic study was investigated with the purified *CmaUPO* using different substrates (ABTS, NBD, and VA) to test its peroxidase and peroxygenase activities, respectively. As presented in Table 1 and Figure S8, the results showed that *CmaUPO* efficiently oxidized VA ($k_{cat} = 378\text{ S}^{-1}$), while displaying a slow, albeit pronounced, catalytic turnover for ABTS. *CmaUPO* exhibited lower K_m values (ranging from approximately 16 to 241 μM) compared with the well-known *AaeUPO* and its variant for both ABTS and NBD (Table 1).⁷ In addition, we compared the kinetic parameters of *CmaUPO* to those of other enzymes reported in the literature. The catalytic efficiency (k_{cat}/K_m) of *CmaUPO* oxidizing ABTS (with a value of 4.72 S⁻¹ μM⁻¹) was found to be higher than that of wild type *PabUPO-I* and *PabUPO-II* due to the higher activity and better binding affinity.¹² Similarly, the k_{cat}/K_m of *CmaUPO* oxidizing NBD (0.61 S⁻¹ μM⁻¹) was higher than that of wild type *AaeUPO*.

Next, to assess the oxidation capacity of *CmaUPO*, we investigated its capability to catalyze the hydroxylation and epoxidation of various substrates (Figures 2 and S9–S13 and Table S2). Notably, ethylbenzene (1), a commonly used substrate for the hydroxylation test, was oxidized with

complete regioselectivity at the benzylic position, yielding 1-phenylethanol (1a and 1b) as the main product but with a poor enantiomeric excess (ee) of 21% (R). In addition, a range of other compounds, including phenol (2), cyclohexane (3), vitamin D₃ (4), and styrene (5), were also tested for their suitability as reaction substrates of *CmaUPO*. Phenol (2) was selectively oxidized to catechol (2a) as a main product. It needs to be pointed out that when 5 mM sodium ascorbate was added in the reaction to avoid phenoxy radical formation, the total turnover number (TTN = 35,609) increased by 65.7% compared to the control experiment, where no sodium ascorbate was used (TTN = 21,494) (Figure S10). Similarly, cyclohexane (3) oxidation by *CmaUPO* yield 8% cyclohexanol (3a) and 92% cyclohexanone (3b). Efficient oxidation of vitamin D₃ (4) produced calcifediol (4a) with high regioselectivity (>99%). Styrene (5) was epoxidized to give styrene oxide (5a and 5b with 28% ee) as the main product in 72% yield, and minor phenylacetaldehyde (5c) was also obtained in 28% yield (Figure 2). In general, these results revealed that *CmaUPO* possessed considerable catalytic potential.

Establishment of a Superfolder-Green-Fluorescent-Protein-Mediated Secretion System in *E. coli*

The broad substrate spectrum and high catalytic potential of *CmaUPO* are evident based on the aforementioned findings. However, its poor enantioselectivity, particularly toward ethylbenzene, necessitates improvement through the selection of an appropriate host cell and the establishment of an effective

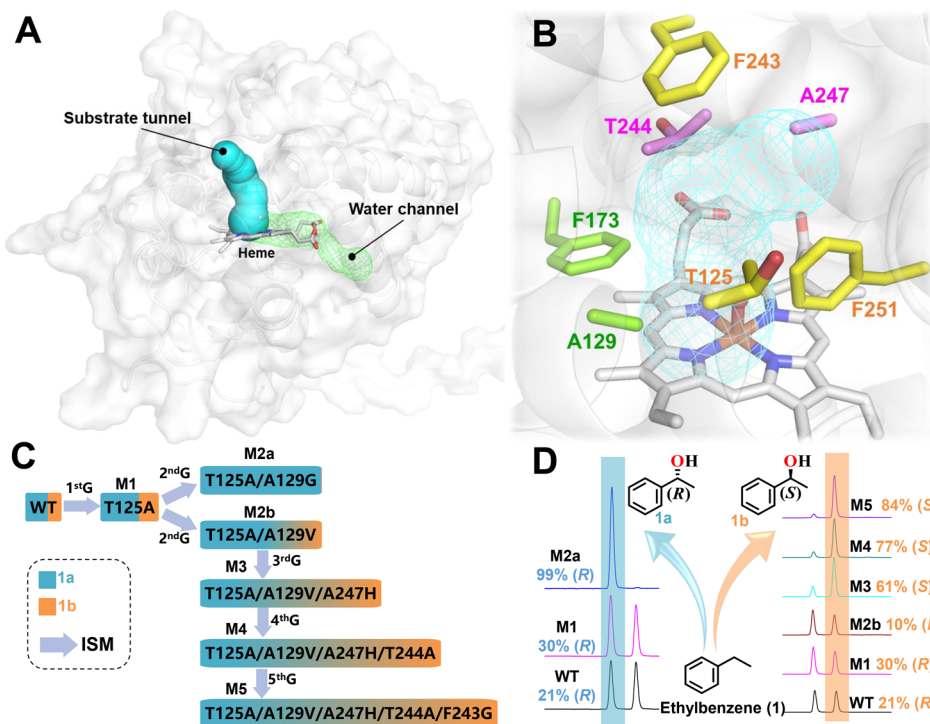


Figure 4. Structure-guided mutagenesis for improving the enantioselectivity of *CmaUPO*. (A) Analysis of protein tunnels using Caver 3.03. Two tunnels were identified as a substrate tunnel (displayed in blue sphere) and potential water/H₂O₂ transport channel (displayed in green mesh), respectively. (B) Zoom of the active sites (lining in the substrate tunnel) around substrate in 5 Å of *CmaUPO*. Within the substrate channel, the residual sites within a 5 Å radius around the substrate sites are divided into three groups. The first group includes the residual sites located at the entrance of the substrate channel (T125, F243, and F251), which are highlighted in yellow. The second group consists of the residual sites on the left side of the substrate in the second layer of the substrate channel (A129 and F173), marked with green. The third group comprises the residual sites on the right side of the substrate in the second layer of the substrate channel (T244 and A247), indicated by violet. Additionally, the substrate tunnel is visualized as a blue mesh. (C) The directed evolution of *CmaUPO* was carried out by ISM. The proportion of blue and orange squares represents the proportion of (R)-1-phenylethanol and (S)-1-phenylethanol products, respectively. (D) Typical GC chromatograms for *CmaUPO* variants catalyzed conversion of ethylbenzene. Reaction conditions: ethylbenzene 10 mM, *CmaUPO* whole cell, glucose 25 mM, glucose oxidase 100 U mL⁻¹, 100 mM potassium phosphate pH 7.5, *V*_{final} = 1 mL, 30 °C, 220 rpm, 10 min. All experiments were performed in triplicates.

directed evolution strategy. *E. coli* is well-known for its efficiency in enzyme engineering, owing to easy scale-up, short turnaround time, and genetic manipulability. Therefore, the first attempt was made to express *CmaUPO* heterologously in *E. coli*. Unfortunately, no protein expression or UPO activity was detected in either the whole cell or lysate supernatant, which is consistent with the previous study where the functional expression of most UPOs in *E. coli* was unsuccessful.¹¹

To overcome this challenge, the use of superfolder green fluorescent protein (*sfGFP*) as a fusion tag has been explored to enhance solubility and promote the secretory expression of heterologous proteins in *E. coli*. With the aid of the *beta*-barrel structure and net negative charge, *sfGFP* serves as a nonsignal peptide to guide protein autosecretion in *E. coli*.^{24–27} The secretion process is divided into three steps: inner membrane translocation, outer membrane anchoring, and extracellular secretion. Large amounts (90%) of protein are anchored at the outer membrane.^{24,25} Given the success of *sfGFP* in previous applications, its potential as a fusion partner for the expression of *CmaUPO* in *E. coli* was investigated. Then, four recombinant vectors, pET23a-*sfGFP-CmaUPO*, pET23a-*CmaUPO-sfGFP*, pET28a-*sfGFP-CmaUPO*, and pET28a-*CmaUPO-sfGFP* with *sfGFP* as a N-terminal or C-terminal fusion protein were constructed, and the resulted plasmids were then transformed into *E. coli* BL21 (DE3) for protein

expression (Figure 3A), hoping to achieve the solubility and secretory expression of *CmaUPO*. After induction with 0.2 mM IPTG at 16 °C for 20 h, both whole cell and lysate supernatant were subjected to activity test using model substrates ABTS and NBD, as well as for catalyzing the hydroxylation of ethylbenzene. As depicted in Figure 3B,C, obvious activity was obtained in the case of *CmaUPO* fused to the C-terminal of *sfGFP* (*sfGFP-CmaUPO*), while no activity was observed when *CmaUPO* was fused to the N-terminal of *sfGFP* (*CmaUPO-sfGFP*). Additionally, it is important to note that the whole cell demonstrated obvious catalytic activity for the first time when supplied with H₂O₂. This might be due to the successful display of *CmaUPO* on the *E. coli* cell surface in its active form. This finding was further supported by the detected activity of membrane protein and intracellular protein of *E. coli* expressing *sfGFP-CmaUPO* (Table S3). Although UPOs such as *MroUPO*, *CviUPO*, and *DcaUPO* have been expressed in an active form in *E. coli*, their applications have been greatly limited by the use of autoinduction medium ZYM-5052, low incubation temperature (16 °C), and extended production duration (4–5 days).^{11,28} In addition, the constructed recombinant cells required lysis to release the enzyme for catalysis. In contrast, our developed secretory expression system allows for enzyme production within 20 h, enabling the first whole-cell-catalyzed reaction of UPOs. Overall, these findings collectively suggest that *sfGFP* can

Table 2. Kinetic Parameters Investigation of *CmaUPO* and its Variants with Ethylbenzene^a

enzymes	K_{cat} (min ⁻¹)	K_m (mM)	K_{cat}/K_m (min ⁻¹ ·mM ⁻¹)	fold ^b
WT	16.3 ± 0.3	6.7 ± 0.4	2.4	
T125A/A129G	76.9 ± 1.5	3.7 ± 0.3	20.9	8.7
T125A-A129V-A247H-T244A-F243G	16.6 ± 0.5	1.6 ± 0.2	10.4	4.3

^aReaction conditions: 2 μM *CmaUPO* or its variants, ethylbenzene (1–50 mM), glucose 25 mM, glucose oxidase 100 U mL⁻¹, 100 mM potassium phosphate pH 7.5, $V_{final} = 500 \mu\text{L}$. The reaction takes place in a metal bath with shaking at 30 °C, 800 rpm for 10 min. All experiments were performed in triplicates. ^bFold was calculated as the ratio of k_{cat}/K_m value between mutants and wild type.

effectively function as a fusion protein to achieve secretory expression of *CmaUPO* in *E. coli*, thereby offering an ideal platform for the efficient directed evolution of *CmaUPO*.

Engineering *CmaUPO* for Enantioselectivity Control

After achieving the heterologous expression of *CmaUPO* in *E. coli*, enzyme engineering was carried out to enhance its enantioselectivity by using hydroxylation of ethylbenzene as a model reaction, since the WT *CmaUPO* displayed only 21% ee in favor of (*R*)-1-phenylethanol as the main product. To start with, homologous modeling was built with AlphaFold2, followed by molecular docking of ethylbenzene into the WT *CmaUPO* (Figure S14). Tunnels, which act as channels, serve to bridge the protein surface with the active site, facilitating efficient molecule transport. They are pivotal in regulating substrate interactions and enabling small molecule access to the active site, which is essential for the enzyme's optimal functionality.²⁹ As presented in Figure 4A, the potential substrate tunnels were analyzed using the Caver 3.03 plugin in PYMOL software,³⁰ based on the molecular docking structure of *CmaUPO* with ethylbenzene (1). This analysis revealed two tunnels traversing the HEME active center (Figure 4A). Of these, only one tunnel connects the protein surface and is identified as the substrate tunnel. Another remaining tunnel is buried within the protein and has narrow tunnel sections, which might be potentially used for water/H₂O₂ transportation. Then, the residual sites T125, A129, F173, F243, T244, A247, and F251 surrounding the ethylbenzene in the substrate access tunnel were targeted for mutagenesis (Figure 4B). First, the NNK-based iterative saturation mutagenesis (ISM)^{31,32} was employed by targeting the substrate channel entrance consisting of T125, F243, and F251 (Figure 4B), the recombinant whole-cell expressing corresponding variants were utilized for the assessment of ethylbenzene hydroxylation. After screening the first round of SM library targeting T125, variant M1 (T125A) was identified with a 2-fold improvement in catalytic activity without affecting the enantioselectivity relative to the wild type, and no improved variants were found in the SM libraries at positions F243 and F251. Subsequently, to improve the (*R*)-enantioselectivity, variant M1 with improved activity was chosen as the parental template to avoid the potential trade-offs, and ISM was performed on a deeper layer of amino acid sites (A129 and F173) within a 5 Å range surrounding the substrate (Figure 4C). Surprisingly, variant M2a (T125A/A129G) was obtained with perfect (*R*)-enantioselectivity (up to 99% ee), and no positive variants was observed in SM library at F173 (Table S4). Clearly, the results demonstrated that A129 plays a crucial role in regulating stereoselectivity.

Next, to switch the enantioselectivity from *R* to *S*, variant M2b (T125A/A129 V), which was identified from the SM library with reduced (*R*)-enantioselectivity from 30% ee (*R*) to 10% ee (*R*), was selected as the parental template (Figure 4D). The residual sites A247, T244, and F243 located on another

side of the substrate were targeted and subjected to ISM. By screening the NNK library at position A247, we successfully identified a triple mutant M3 (T125A/A129V/A247H), which reversed enantioselectivity and produced (*S*)-1-phenylethanol as the dominated product with 61% ee (*S*) (Figure 4D and Table S5). Further mutagenesis targeted residual site T244, leading to a variant M4 (T125A/A129V/A247H/T244A), which showed enhanced (*S*)-1-phenylethanol selectivity of up to 77% ee (*S*). Finally, based on variant M4, variant M5 (T125A/A129V/A247H/T244A/F243G) was obtained by mutating F to G at position 243, which further enhanced the enantiomeric excess to 84% ee (*S*) (Figure 4C and Table S5). To our knowledge, variant M5 represents the highest (*S*)-enantioselectivity for UPOs catalyzed benzylic hydroxylation of ethylbenzene, surpassing all the reported natural UPOs or their variants [GdiUPO-II: 61% ee (*S*), CabUPO-V: 20% ee (*S*), AaeUPO variant d28: 32% ee (*S*), and AbrUPO: 20% ee (*S*)].^{15,33,34}

Subsequently, the two *CmaUPO* variants M2a and M5 were extracellularly expressed in *P. pastoris* X33, and the enzyme was then purified and employed for kinetic study. It was found that both variants exhibited higher catalytic efficiency (k_{cat}/K_m) compared to that of WT *CmaUPO* (Table 2 and Figure S15). Variant M2a demonstrated the most superior catalytic performance ($k_{cat}/K_m = 20.9 \text{ min}^{-1} \text{ M}^{-1}$), which was 8.7-fold higher than that of WT *CmaUPO*, while the catalytic efficiency of variant M5 ($k_{cat}/K_m = 10.4 \text{ min}^{-1} \text{ M}^{-1}$) was also approximately 4.3-fold higher relative to that of WT *CmaUPO*. It is noteworthy that the enantioselectivities of both variants expressed from *P. pastoris* remained consistent with the enzymes produced from the prokaryotic host *E. coli*, indicating that the catalytic selectivity of UPOs is unaffected by the expression host.

Thus, based on the superfolder-green-fluorescent-protein-mediated secretion system using *E. coli* as the host cell, the engineering of *CmaUPO* was successfully conducted with ISM by targeting the hotspot residues located in the substrate access tunnel. Consequently, variants with both improved activity and enantioselectivity were obtained with limited screening effort and short time, which show great advantages over the yeast-based engineering system, for which prolonged heterologous production and the complexity of mutant operations are inevitably needed. Theoretically, in addition to ethylbenzene, further engineering of *CmaUPO* for other substrates could also be achieved with the developed system.

Computational Analysis for *CmaUPO* and its Variants Catalyzed Hydroxylation of Ethylbenzene

To understand the molecular mechanisms underlying the altered enantioselectivity of *CmaUPO*-catalyzed ethylbenzene hydroxylation, we performed structural and computational analyses. First, the homology models of *CmaUPO* mutants (M2a and M5) were built for structural analysis. Compared with wildtype *CmaUPO*, the results revealed that the mutation

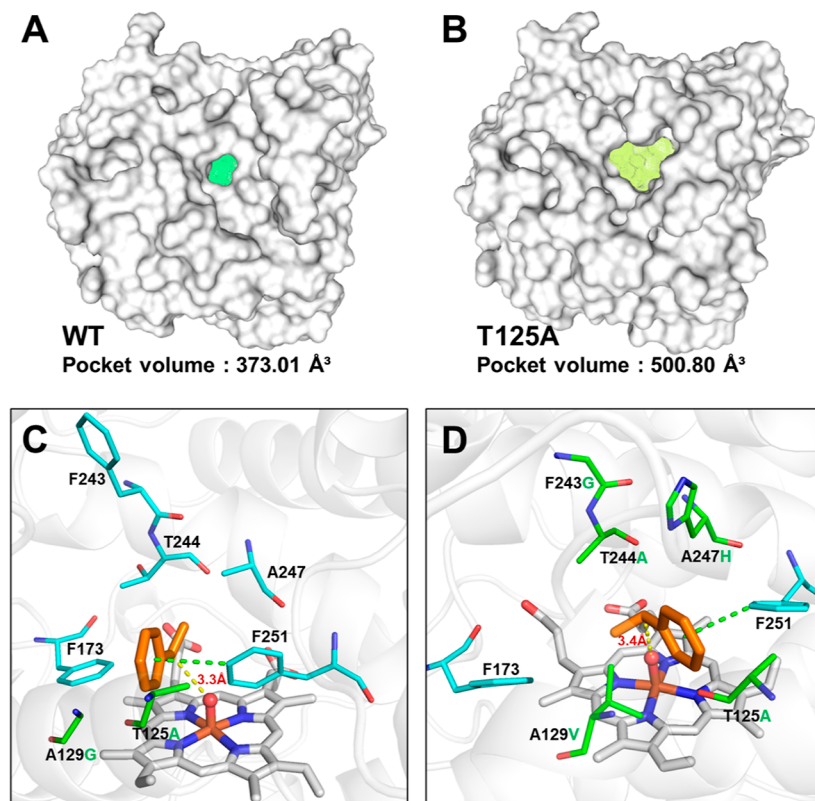


Figure 5. Structural analysis and molecular docking of *CmaUPO* and its variants with ethylbenzene. (A) The surface structure of the active pocket inlet and active pocket volume diagram of WT *CmaUPO*. The volume of the active pocket is 373.01 \AA^3 . The volume was measured using the DoGSiteScorer tool of the ProteinsPlus platform (<https://proteins.plus/>).³⁵ (B) The surface structure of the active pocket inlet and active pocket volume diagram of variant T125A. The volume of the active pocket is 500.80 \AA^3 . (C) Zoom of the active site of variant M2a (T125A/A129G). Key sites are marked in light blue sticks (target mutant residues marked in green) and labeled in black for mutant T125A/A129G. The substrate ethylbenzene is show in orange. (D) Zoom of the active site of variant M5 (T125A/A129V/A247H/T244A/F243G). Key sites are depicted using light blue sticks, with target mutant residues highlighted in green and labeled in black. The substrate ethylbenzene is represented in orange.

T125A, occurred at the substrate tunnel entrance in both variants, resulted in a wider channel and a larger pocket (500.80 \AA^3), making it considerably easier for the substrate to access the active pocket (Figure 5A,B). Furthermore, the substitution of threonine with alanine increased the hydrophobicity of the active pocket, which is a crucial factor in accommodating the hydrophobic substrate and facilitating its transformations.

Next, we performed a docking analysis on *CmaUPO* and its variants. For WT, the docking results show that the conformation of the substrate ethylbenzene is slightly parallel to the heme ring due to the hydrophobic interactions formed between phenyl and ethyl groups of **1** with A129 and F173, respectively. Therefore, the distance between the C7 carbon of ethylbenzene and the heme oxygen atom (heme-O) is 3.7 \AA , and the corresponding angles are $\text{O}(\text{Fe}=\text{O})-(\text{Eth})-\text{H}(\text{C}_{7R})-(\text{Eth})-\text{C}$ (7) and $\text{O}(\text{Fe}=\text{O})-(\text{Eth})-\text{H}(\text{C}_{7S})-(\text{Eth})-\text{C}$ (7) at 123 and 97.3° , respectively (Figures S14 and S16). These results suggest that WT exhibits poor stereoselectivity in hydroxylating ethylbenzene, which is consistent with experimental results. Notably, for variant M2a, the T125A/A129G mutation resulted in a reorientation of the phenyl plane of ethylbenzene, causing **1** to adopt a perpendicular conformation to the heme plane (Figure 5C). This may be due to the replacement of Ala by Gly at position A129, which creates more space for substrate conformational rotation. Moreover, the lack of the methyl side chain causes the phenyl group of

the substrate to rotate, enabling $\pi-\pi$ stacking interaction with F251 and further stabilizing the substrate configuration. This results in a distance of 3.3 \AA between the C7 atom of the substrate and the O atom of heme, with an angle of $\text{O}(\text{Fe}=\text{O})-(\text{Eth})-\text{H}(\text{C}_{7R})-(\text{Eth})-\text{C}$ (7) became 156.6° (Figure S16), leading to (R)-1-phenylethanol as the sole hydroxylation product (Figure 5C).

For variant M5 (T125A/A129V/A247H/T244A/F243G), the phenyl group of the substrate is closer to F251 compared to M2a, and the ethyl group undergoes a counterclockwise rotation, bringing the hydrogen atom at the C_{7S} position closer to the iron–oxygen (Figures 5D and S16). This may be due to the A129 V mutation pushing the substrate phenyl group away and the introduction of A247H mutation causing the substrate ethyl to flip. The $\pi-\pi$ stacking interaction provided by F251 stabilizes the phenyl moiety of the substrate (Figure 5D). Therefore, the distance between the C7 atom of substrate **1** and the O atom of heme is 3.4 \AA , and the angle of the $\text{O}(\text{Fe}=\text{O})-(\text{Eth})-\text{H}(\text{C}_{7S})-(\text{Eth})-\text{C}$ (7) is 126.1° , which favors the S-type attack conformation of ethylbenzene (Figure 5D). These findings provide valuable insights into the mechanism of *CmaUPO* catalyzed selective activation of inert C–H bond, providing guidance for further engineering of UPOs in various chemical transformations.

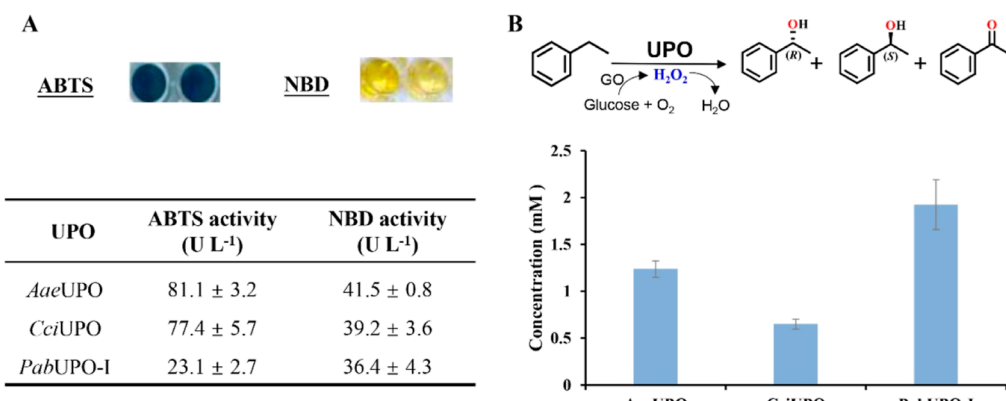


Figure 6. Versatility of the fusion-expression platform for other UPOs. (A) Lysate supernatant activities of UPOs measured with ABTS and NBD. (B) Asymmetric hydroxylation of ethylbenzene using recombinant *E. coli* cells expressing corresponding UPOs.

Generality of *E. coli* sfGFP-Mediated Secretion System for Other UPOs

To demonstrate the generality of the *E. coli* sfGFP-mediated secretion system, three different UPOs, including *AaeUPO*, *CciUPO* and *PabUPO-I*, were individually investigated. The cell lysate of recombinant *E. coli* expressing the UPO was then subjected to an activity test using model substrates ABTS and NBD. Notably, all tested UPOs exhibited obvious activity, particularly *AaeUPO* and *CciUPO*, indicating successful heterologous expression using the *E. coli* sfGFP-mediated secretion system (Figure 6A). Furthermore, whole-cell expression of the corresponding UPO as a catalyst was then employed in the hydroxylation of ethylbenzene (Figure 6B). The results showed that all whole cells demonstrated catalytic ability, suggesting that these enzymes could be expressed and displayed well on the *E. coli* cell surface in its active form. Then, the expression levels were determined for the sfGFP-fused UPOs (*CmaUPO*, *AaeUPO*, *CciUPO*, and *PabUPO-I*). Consequently, protein expression ranging from 14.6 to 16.3 mg L^{-1} were achieved, which are higher than most of the existing *E. coli* systems for other UPOs' expression (Table S5).^{11,21,36} In contrast, UPOs without sfGFP fusion showed no activity for ethylbenzene hydroxylation. Overall, the *E. coli* sfGFP-mediated secretion system presents a valuable platform for facilitating UPO secretion expression in *E. coli*, and it should be considered a significant tool for screening novel UPOs and evolving the existing UPOs to improve their catalytic properties.

CONCLUSIONS

In summary, by enzyme mining, a novel *CmaUPO* from *C. marcescens* was discovered, showing a significant catalytic potential for hydroxylation and epoxidation. Focusing on *CmaUPO*, we established an efficient *E. coli* cell surface-displayed secretory expression system using the sfGFP-mediated method, which is ideal for UPO expression and directed evolution. This system also enables UPOs exposure to H_2O_2 , enabling whole-cell catalysis of UPO for the first time. Compared to reported UPO catalysis from *E. coli* and yeast expression, this system offers advantages such as no cell lysis, low-cost culturing, and short turnaround time. Furthermore, this system further facilitated the engineering of *CmaUPO* [21% ee (R) for WT], leading to improved ethylbenzene enantioselectivity oxyfunctionalization. Two variants with greatly improved enantioselectivities were obtained: one

generated the (R)-1-phenylethanol with 99% ee (R), and the other produced (S)-1-phenylethanol with 84% ee (S), representing the best (S)-selectivity achieved for UPOs catalyzed hydroxylation of ethylbenzene to date. Additionally, the cell lysate activities of three recombinant UPOs (*AaeUPO*, *CciUPO*, and *PabUPO-I*) and the corresponding whole-cell hydroxylation of ethylbenzene demonstrated the versatility of the sfGFP-mediated secretion system. Consequently, this developed system provides a robust platform for heterologous expression and enzyme engineering of UPOs, indicating great potential for their sustainable and efficient applications in various chemical transformations.

ASSOCIATED CONTENT

Supporting Information

The Supporting Information is available free of charge at <https://pubs.acs.org/doi/10.1021/jacsau.4c00129>.

Experimental information and procedures, screening of UPO candidates, GC and HPLC analysis, comparison of membrane proteins and intracellular proteins, comparison of UPOs heterologous expression, SDS-PAGE results, pH activity profiles, sensitivity of *CmaUPO* toward hydrogen peroxide, H_2O_2 tolerance, thermal inactivation assay, thermodynamic stability, solvent tolerance, Michaelis–Menten curves, stacked GC-FID traces, stacked HPLC traces, active site of WT *CmaUPO*, steady-state kinetic behavior, mapping of substrate 1, and nucleotide sequence information (PDF)

AUTHOR INFORMATION

Corresponding Authors

Lixin Kang – State Key Laboratory of Biocatalysis and Enzyme Engineering, Hubei Key Laboratory of Industrial Biotechnology, School of Life Sciences, Hubei University, Wuhan 430062, P. R. China; Email: lixinkang2007@hubu.edu.cn

Aitao Li – State Key Laboratory of Biocatalysis and Enzyme Engineering, Hubei Key Laboratory of Industrial Biotechnology, School of Life Sciences, Hubei University, Wuhan 430062, P. R. China; orcid.org/0000-0001-6036-4058; Email: aitaoli@hubu.edu.cn

Authors

Xingyu Yan – State Key Laboratory of Biocatalysis and Enzyme Engineering, Hubei Key Laboratory of Industrial Biotechnology, School of Life Sciences, Hubei University, Wuhan 430062, P. R. China

Xiaodong Zhang – State Key Laboratory of Biocatalysis and Enzyme Engineering, Hubei Key Laboratory of Industrial Biotechnology, School of Life Sciences, Hubei University, Wuhan 430062, P. R. China

Haoran Li – State Key Laboratory of Biocatalysis and Enzyme Engineering, Hubei Key Laboratory of Industrial Biotechnology, School of Life Sciences, Hubei University, Wuhan 430062, P. R. China

Di Deng – State Key Laboratory of Biocatalysis and Enzyme Engineering, Hubei Key Laboratory of Industrial Biotechnology, School of Life Sciences, Hubei University, Wuhan 430062, P. R. China

Zhiyong Guo – State Key Laboratory of Biocatalysis and Enzyme Engineering, Hubei Key Laboratory of Industrial Biotechnology, School of Life Sciences, Hubei University, Wuhan 430062, P. R. China

Complete contact information is available at:
<https://pubs.acs.org/10.1021/jacsau.4c00129>

Author Contributions

[†]X.Y., X.Z., and H.L. contributed equally to this work. A.L. and L.K. conceived and supervised this project. X.Y., X.Z., H.L., D.D., and Z.G. were involved carrying out the experiment, data reduction, drafted the manuscript, performed the mechanism study, and analyzed the data; all authors read, approved, and modified the final manuscript. CRediT: Xingyu Yan data curation, formal analysis, methodology, writing-original draft; Xiaodong Zhang formal analysis, methodology, visualization, writing-original draft; Haoran Li formal analysis, methodology, writing-original draft; Di Deng formal analysis, visualization; Lixin Kang conceptualization, methodology, writing-original draft; Aitao Li conceptualization, project administration, writing-review & editing.

Funding

This work was funded by the National Key Research and Development Program of China (2021YFC2102700) and was supported by the Key Science and Technology Innovation Project of Hubei Province (2021BAD001) as well as the Research Program of State Key Laboratory of Biocatalysis and Enzyme Engineering.

Notes

The authors declare no competing financial interest.

ACKNOWLEDGMENTS

We thank Professor Dr. Lixin Ma of the Hubei University for providing the plasmids of pET23a-sfGFP15 and pET28a-sfGFP15.

REFERENCES

- (1) Hofrichter, M.; Kellner, H.; Herzog, R.; Karich, A.; Liers, C.; Scheibner, K.; Kimani, V.; Ullrich, R. Fungal peroxygenases: a phylogenetically old superfamily of heme enzymes with promiscuity for oxygen transfer reactions. In *Grand Challenges in Fungal Biotechnology*; Springer International Publishing, 2020; pp 369–403..
- (2) Hobisch, M.; Holtmann, D.; Gomez de Santos, P.; Alcalde, M.; Hollmann, F.; Kara, S. Recent developments in the use of peroxygenases-exploring their high potential in selective oxyfunctionalizations. *Biotechnol. Adv.* **2021**, *51*, 107615.
- (3) Bormann, S.; Gomez Baraibar, A.; Ni, Y.; Holtmann, D.; Hollmann, F. Specific oxyfunctionalisations catalysed by peroxygenases: opportunities, challenges and solutions. *Catal. Sci. Technol.* **2015**, *5*, 2038–2052.
- (4) Wang, Y.; Lan, D.; Durrani, R.; Hollmann, F. Peroxygenases enroute to becoming dream catalysts. What are the opportunities and challenges? *Curr. Opin. Chem. Biol.* **2017**, *37*, 1–9.
- (5) Ullrich, R.; Nüske, J.; Scheibner, K.; Spantzel, J.; Hofrichter, M. Novel haloperoxidase from the agaric basidiomycete *Agrocybe aegerita* oxidizes aryl alcohols and aldehydes. *Appl. Environ. Microbiol.* **2004**, *70*, 4575–4581.
- (6) Ullrich, R.; Poraj-Kobielska, M.; Scholze, S.; Halbout, C.; Sandvoss, M.; Pecyna, M. J.; Scheibner, K.; Hofrichter, M. Side chain removal from corticosteroids by unspecific peroxygenase. *J. Inorg. Biochem.* **2018**, *183*, 84–93.
- (7) Molina-Espeja, P.; Garcia-Ruiz, E.; Gonzalez-Perez, D.; Ullrich, R.; Hofrichter, M.; Alcalde, M. Directed evolution of unspecific peroxygenase from *Agrocybe aegerita*. *Appl. Environ. Microbiol.* **2014**, *80*, 3496–3507.
- (8) Hofrichter, M.; Ullrich, R. Oxidations catalyzed by fungal peroxygenases. *Curr. Opin. Chem. Biol.* **2014**, *19*, 116–125.
- (9) Gröbe, G.; Ullrich, R.; Pecyna, M. J.; Kapturska, D.; Friedrich, S.; Hofrichter, M.; Scheibner, K. High-yield production of aromatic peroxygenase by the agaric fungus *Marasmius rotula*. *AMB Express* **2011**, *1*, 31.
- (10) Kiebist, J.; Schmidtke, K. U.; Zimmermann, J.; Kellner, H.; Jehmlich, N.; Ullrich, R.; Zander, D.; Hofrichter, M.; Scheibner, K. A peroxygenase from *Chaetomium globosum* catalyzes the selective oxygenation of testosterone. *ChemBioChem* **2017**, *18*, 563–569.
- (11) Linde, D.; Olmedo, A.; Gonzalez-Benjumea, A.; Estevez, M.; Renau-Minguez, C.; Carro, J.; Fernandez-Fueyo, E.; Gutierrez, A.; Martinez, A. T. Two new unspecific peroxygenases from heterologous expression of fungal genes in *Escherichia coli*. *Appl. Environ. Microbiol.* **2020**, *86*, No. e02899-19.
- (12) Gomez de Santos, P.; Hoang, M. D.; Kiebist, J.; Kellner, H.; Ullrich, R.; Scheibner, K.; Hofrichter, M.; Liers, C.; Alcalde, M. Functional expression of two unusual acidic peroxygenases from *Candidoomyces aberdarensis* in yeasts by adopting evolved secretion mutations. *Appl. Environ. Microbiol.* **2021**, *87*, No. e0087821.
- (13) Rotilio, L.; Swoboda, A.; Ebner, K.; Rinnofner, C.; Glieder, A.; Kroutil, W.; Mattevi, A. Structural and biochemical studies enlighten the unspecific peroxygenase from *Hypoxyylon* sp. EC38 as an efficient oxidative biocatalyst. *ACS Catal.* **2021**, *11*, 11511–11525.
- (14) Ma, Y.; Liang, H.; Zhao, Z.; Wu, B.; Lan, D.; Hollmann, F.; Wang, Y. A novel unspecific peroxygenase from *Galatina marginata* for biocatalytic oxyfunctionalization reactions. *Mol. Catal.* **2022**, *531*, 112707.
- (15) Schmitz, F.; Koschorreck, K.; Hollmann, F.; Urlacher, V. B. Aromatic hydroxylation of substituted benzenes by an unspecific peroxygenase from *Aspergillus brasiliensis*. *React. Chem. Eng.* **2023**, *8*, 2177–2186.
- (16) Qu, G.; Li, A.; Acevedo-Rocha, C. G.; Sun, Z.; Reetz, M. T. The crucial role of methodology development in directed evolution of selective enzymes. *Angew. Chem., Int. Ed.* **2020**, *59*, 13204–13231.
- (17) Molina-Espeja, P.; Cañellas, M.; Plou, F. J.; Hofrichter, M.; Lucas, F.; Guallar, V.; Alcalde, M. Synthesis of 1-naphthol by a natural peroxygenase engineered by directed evolution. *ChemBioChem* **2016**, *17*, 341–349.
- (18) Martin-Diaz, J.; Molina-Espeja, P.; Hofrichter, M.; Hollmann, F.; Alcalde, M. Directed evolution of unspecific peroxygenase in organic solvents. *Biotechnol. Bioeng.* **2021**, *118*, 3002–3014.
- (19) Knorrseidt, A.; Soler, J.; Hünecke, N.; Püllmann, P.; García-Borràs, M.; Weissenborn, M. J. Accessing chemo- and regioselective benzylic and aromatic oxidations by protein engineering of an unspecific peroxygenase. *ACS Catal.* **2021**, *11*, 7327–7338.
- (20) Carro, J.; González-Benjumea, A.; Fernández-Fueyo, E.; Aranda, C.; Guallar, V.; Gutiérrez, A.; Martínez, A. T. Modulating

fatty acid epoxidation vs hydroxylation in a fungal peroxygenase. *ACS Catal.* **2019**, *9*, 6234–6242.

(21) Robinson, W. X. Q.; Mielke, T.; Melling, B.; Cuetos, A.; Parkin, A.; Unsworth, W. P.; Cartwright, J.; Grogan, G. Comparing the catalytic and structural characteristics of a “short” unspecific peroxygenase (UPO) expressed in *Pichia pastoris* and *Escherichia coli*. *ChemBioChem* **2023**, *24*, No. e202200558.

(22) Kinner, A.; Rosenthal, K.; Lütz, S. Identification and expression of new unspecific peroxygenases—recent advances, challenges and opportunities. *Front. Bioeng. Biotechnol.* **2021**, *9*, 705630.

(23) Ebner, K.; Pfeifenberger, L. J.; Rinnofner, C.; Schusterbauer, V.; Glieder, A.; Winkler, M. Discovery and heterologous expression of unspecific peroxygenases. *Catalysts* **2023**, *13*, 206.

(24) Zhang, Z.; Tang, R.; Zhu, D.; Wang, W.; Yi, L.; Ma, L. Non-peptide guided auto-secretion of recombinant proteins by super-folder green fluorescent protein in *Escherichia coli*. *Sci. Rep.* **2017**, *7*, 6990.

(25) Liu, M.; Wang, B.; Wang, F.; Yang, Z.; Gao, D.; Zhang, C.; Ma, L.; Yu, X. Soluble expression of single-chain variable fragment (scFv) in *Escherichia coli* using superfolder green fluorescent protein as fusion partner. *Appl. Microbiol. Biotechnol.* **2019**, *103*, 6071–6079.

(26) Xia, J.; Xin, W.; Wang, F.; Xie, W.; Liu, Y.; Xu, J. Cloning and characterization of fructose-1,6-bisphosphate aldolase from *Euphausia superba*. *Int. J. Mol. Sci.* **2022**, *23*, 10478.

(27) Bilgin, S. Expression strategy of soluble recombinant human TGF- β 3 in *Escherichia coli*: sfGFP-Fusion Tag. *Sak. Univ. J. Sci.* **2023**, *27*, 204–213.

(28) Studier, F. W. Protein production by auto-induction in high-density shaking cultures. *Protein Expr. Purif.* **2005**, *41*, 207–234.

(29) Kokkonen, P.; Bednar, D.; Pinto, G.; Prokop, Z.; Damborsky, J. Engineering enzyme access tunnels. *Biotechnol. Adv.* **2019**, *37*, 107386.

(30) Chovancova, E.; Pavelka, A.; Benes, P.; Strnad, O.; Brezovsky, J.; Kozlikova, B.; Gora, A.; Suštr, V.; Klvaňa, M.; Medek, P.; Biedermannova, L.; Sochor, J.; Damborsky, J. CAVER 3.0: a tool for the analysis of transport pathways in dynamic protein structures. *PLoS Comput. Biol.* **2012**, *8*, No. e1002708.

(31) Reetz, M. T.; Carballeira, J. D. Iterative saturation mutagenesis (ISM) for rapid directed evolution of functional enzymes. *Nat. Protoc.* **2007**, *2*, 891–903.

(32) Acevedo-Rocha, C. G.; Hoebenreich, S.; Reetz, M. T. Iterative saturation mutagenesis: a powerful approach to engineer proteins by systematically simulating Darwinian evolution. *Methods Mol. Biol.* **2014**, *1179*, 103–128.

(33) Gomez de Santos, P.; Mateljak, I.; Hoang, M. D.; Fleishman, S. J.; Hollmann, F.; Alcalde, M. Repertoire of computationally designed peroxygenases for enantiodivergent C–H oxyfunctionalization reactions. *J. Am. Chem. Soc.* **2023**, *145*, 3443–3453.

(34) Swoboda, A.; Pfeifenberger, L. J.; Duhović, Z.; Bürgler, M.; Oroz-Guinea, I.; Bangert, K.; Weißenseiner, F.; Parigger, L.; Ebner, K.; Glieder, A.; Kroutil, W. Enantioselective high-throughput assay showcased for the identification of (R)- as well as (S)-selective unspecific peroxygenases for C–H oxidation. *Angew. Chem., Int. Ed.* **2023**, *62*, No. e202312721.

(35) Schöning-Stierand, K.; Diedrich, K.; Ehrt, C.; Flachsenberg, F.; Graef, J.; Sieg, J.; Penner, P.; Poppinga, M.; Ungethüm, A.; Rarey, M. ProteinsPlus: a comprehensive collection of web-based molecular modeling tools. *Nucleic Acids Res.* **2022**, *50*, W611–W615.

(36) González-Benjumea, A.; Carro, J.; Renau-Mínguez, C.; Linde, D.; Fernández-Fueyo, E.; Gutiérrez, A.; Martínez, A. T. Fatty acid epoxidation by *Collariella virescens* peroxygenase and heme-channel variants. *Catal. Sci. Technol.* **2020**, *10*, 717–725.

CAS BIOFINDER DISCOVERY PLATFORM™

ELIMINATE DATA SILOS. FIND WHAT YOU NEED, WHEN YOU NEED IT.

A single platform for relevant, high-quality biological and toxicology research

Streamline your R&D

CAS A division of the American Chemical Society